

# Kernel-Based Regularized Continuous-Time System Identification from Sampled Data

Xiaozhu Fang, Biqiang Mu, and Tianshi Chen

**Abstract**—The identification of continuous-time (CT) systems from discrete-time (DT) input and output signals, i.e., the sampled data, has received considerable attention for half a century. The state-of-the-art methods are parametric methods and thus subject to the typical issues of parametric methods. In the last decade, a major advance in system identification is the so-called kernel-based regularization method (KRM), which is free of the issues of parametric methods. It is interesting to test the potential of KRM on CT system identification. However, very few results have been reported, mainly because the estimators of KRM have no closed forms for general CT input signals, except for some very special cases. In this paper, we show for KRM that the estimators have closed forms when the DT input signal has the typical intersample behavior, i.e., zero-order hold or band-limited, and this paves the way for the application of KRM for CT system identification. Numerical simulations show that the proposed method is more robust than the state-of-the-art methods and more accurate when the sample size is small.

## I. INTRODUCTION

Continuous-time (CT) systems have received increasing interest due to their association with the natural world and physical processes through derivatives, integrals, and differential equations. The identification of CT systems from the discrete-time (DT) input and output signals (which are also called sampled data) has been a long-standing topic for half a century, see survey papers [1]–[3]. The existing methods can be divided into two classes: indirect ones and direct ones, see e.g., [2], [3]. Specifically, the direct methods identify a CT parametric model directly from the sampled data, while the indirect methods first identify a DT model from the sampled data, and then convert it to a CT parametric model. The choice between direct methods and indirect methods has been controversial for decades, and recently, the mainstream has been the direct methods. Particularly, the state-of-the-art direct methods are the Simplified Refined Instrumental Variable method for Continuous-time system (SRIVC) [4], [5], and the Maximum Likelihood/Prediction Error Method (ML/PEM) [6], [7]. However, due to the use of

parametric models, both SRIVC and ML/PEM are subject to the typical issues of parametric methods. First, the model order should be decided in advance, and the problem of finding a suitable model order is challenging, especially when the data is short and/or has a low signal-to-noise ratio. Second, when estimating a model with a large order, the nonconvex optimization problem involved in the parameter estimation often has severe local minima issues, leading to large variations between the different noise realizations, see [7, Sec. 6.5].

In the last decade, a major advance in system identification is the so-called kernel-based regularization method (KRM). It is free of the aforementioned issues of parametric methods, and moreover, extensive numerical and experimental simulation results have shown that, for DT system identification, KRM can provide more accurate and robust DT model estimates than ML/PEM when the data is short and/or has a low signal-to-noise ratio, and KRM has become an emerging paradigm in system identification [8]. The success of KRM in DT system identification naturally encourages researchers to further explore whether such success can be copied in CT system identification. There have been some attempts recently, see e.g. [9], [10]. However, the integral involved in the computation of the predicted output has no closed form, leading to the absence of the closed form of the estimators. An accurate approximation of the integral is feasible but expensive, and thus KRM has not been essentially tested for CT system identification, except for some very special cases, e.g. the input is an impulse or step signal [10], [11].

In this paper, we apply KRM to CT system identification from the sampled data with extra knowledge of the input behaviour. Specifically, we convert the DT input signal into a CT input signal by exploiting the given intersample behavior, e.g. zero-order-hold (ZOH) and band-limited (BL). Moreover, KRM also needs to access to the past input, which is unknown in the sampled data; as a result, the past behavior of the input signal needs to be assumed, e.g. periodically appended (PA) or zero appended (ZA), and the inconsistency of this assumption is also modeled as the transient error, see e.g. [12], [13]. Consequently, KRM can be adopted for the sampled data, and notably, we have found that the closed forms of the estimators exist for certain combinations of the intersample and past behaviors: ZOH and PA, ZOH and ZA, BL and PA, which enables the efficient and accurate implementation of KRM. Lastly, we run numerical simulations to compare the proposed methods with SRIVC and ML/PEM, where the proposed method not only has better robustness but also, when the sample size is

This work was funded by NSFC under contract No. 62273287, Shenzhen Science and Technology Innovation Commission under contract No. JCYJ20220530143418040, the Thousand Youth Talents Plan funded by the central government of China, and the National Key R&D Program of China under contract No. 2022YFA1004700.

Xiaozhu Fang and Tianshi Chen are with School of Data Science and Shenzhen Research Institute of Big Data, The Chinese University of Hong Kong, Shenzhen, 518172 China (email: xiaozhufang@link.cuhk.edu.cn, tschen@cuhk.edu.cn)

Biqiang Mu is with the Key Laboratory of Systems and Control of CAS, Institute of Systems Science, Academy of Mathematics and System Science, Chinese Academy of Sciences, Beijing 100190, China (email: bqmu@amss.ac.cn)

small, has higher accuracy.

The remaining part of this paper is organized as follows. In Section II, CT system identification and KRM are briefly reviewed. In Section III, KRM is applied to CT system identification from the sampled data, and the results are also extended to the unknown past behavior. Lastly, numerical simulations are shown in Section IV. The proofs of the propositions and lemmas are skipped unless otherwise stated.

## II. BACKGROUND AND PROBLEM STATEMENT

### A. CT System Identification from the Sampled Data

Consider a bounded-input-bounded-output (BIBO) stable, strictly causal, continuous-time (CT), single-input single-output (SISO), and linear time-invariant (LTI) system, described by

$$y(t) = y_0(t) + v(t), \quad y_0(t) = \int_0^\infty u(t-\tau)g(\tau)d\tau, \quad (1)$$

where  $t, \tau \in \mathbb{R}$  are time indexes,  $u(t), y(t) \in \mathbb{R}$  are the input and output of the system, respectively,  $v(t) \in \mathbb{R}$  is the disturbance,  $g(\tau) \in \mathbb{R}$  is the impulse response of the system, and  $y_0(t) \in \mathbb{R}$  is the noiseless output, i.e., the convolution between the impulse response  $g(\cdot)$  and the input  $u(\cdot)$  evaluated at time  $t$ .

Let  $u(t)$  and  $y(t)$  sampled at  $t = 0, T_s, \dots, (N-1)T_s$ , where  $T_s$  is the sampling interval. Since  $y(t)$  is sampled, the disturbance  $v(t)$  can be characterized by a discrete-time (DT) model [14, Sec. 2.2], and, moreover,  $v(t)$  is assumed to be white Gaussian distributed with mean zero and variance  $\sigma^2$ , independent of  $u(t)$ .

Our goal is to identify the CT impulse response  $g(\tau)$  from the sampled data, i.e.,  $N$  sampled measurement of the input and output  $\{u(kT_s), y(kT_s)\}_{k=0}^{N-1}$ .

### B. Kernel-Based Regularization Method

Recently, the kernel-based regularization method (KRM) has been intensively discussed in the context of system identification. KRM has been applied to CT system identification from the CT input signal  $\{u(t)\}_{t \leq NT_s}$  and DT output signal  $\{y(kT_s)\}_{k=0}^{N-1}$ , see e.g. [9], [10]. Specifically, the CT impulse response  $\hat{g}$  is estimated by the regularized Least Squares as

$$\hat{g} = \arg \min_{g \in \mathcal{H}_g} \sum_{k=0}^{N-1} \left| y(kT_s) - \int_0^\infty u(kT_s - \tau)g(\tau)d\tau \right|^2 + \gamma \|g\|_{\mathcal{H}_g}^2 \quad (2)$$

where  $\gamma \geq 0$  is the regularization parameter, and  $\mathcal{H}_g$  is a reproducing kernel Hilbert spaces induced by the kernel  $\kappa_g : \mathbb{R} \times \mathbb{R} \rightarrow \mathbb{R}$ . It is well-known that  $\hat{g}$  in (2) can be obtained from the representer theorem [9], leading to the following matrix-vector form:

$$\hat{g}(\tau) = \mathbf{\Sigma}_{gy_0}(\tau)(\mathbf{\Sigma}_{y_0} + \gamma I_N)^{-1} \mathbf{y}, \quad (3)$$

$$\begin{cases} \mathbf{\Sigma}_{y_0} = \int_0^\infty \int_0^\infty u(\mathbf{t}-\tau)u(\mathbf{t}-\tau')\kappa_g(\tau, \tau') d\tau d\tau', \\ \mathbf{\Sigma}_{gy_0}(\tau) = \int_0^\infty u(\mathbf{t}^T - \tau')\kappa_g(\tau, \tau')d\tau', \end{cases} \quad (4)$$

where  $\mathbf{y} = [y(0), \dots, y((N-1)T_s)]^T$ ,  $I_N$  is a  $N \times N$  identity matrix,  $\mathbf{t} = [0, \dots, (N-1)T_s]^T$  with  $\mathbf{t}^T$  denoting

its transpose, and the notation of vectorized scalar functions is employed above<sup>1</sup>.

It should be noted that the solution (3) can also be interpreted as a maximum a posteriori (MAP) estimate in the following Bayesian framework.

**Lemma 1 ([9]):** Consider (1) with:

- 1)  $g(\tau)$  is a zero-mean Gaussian process with covariance function  $\kappa_g(\tau, \tau')$ ,
- 2)  $v(t)$  is a white Gaussian noise with variance  $\sigma^2 = \gamma$ , independent with  $g(\tau)$ .

Given observation  $\mathbf{y} = [y(0), \dots, y((N-1)T_s)]^T$ , the MAP estimate of  $g(\tau)$  coincides with (3).

It should be noted that the estimator (3) has the matrix-vector form, and then (3) has the closed form if matrices  $\mathbf{\Sigma}_{gy_0}(\tau)$  and  $\mathbf{\Sigma}_{y_0}$  have closed forms. Nonetheless, for general  $u(t)$ , matrices  $\mathbf{\Sigma}_{gy_0}(\tau)$  and  $\mathbf{\Sigma}_{y_0}$  have no closed form due to the infinite-dimensional integral. Though numerical integral techniques can be employed, the computation would be either inaccurate or expensive. Thus, the absence of the closed forms of  $\mathbf{\Sigma}_{gy_0}(\tau)$  and  $\mathbf{\Sigma}_{y_0}$  has been the main barrier of the applications of KRM.

**Remark 1:** The closed form of  $\mathbf{\Sigma}_{y_0}$  also influences the hyperparameter estimation, e.g. the marginal likelihood [9], in the same manner.

### C. Problem Statement

In what follows, we consider KRM for CT system identification from the sampled data. The idea is straightforward by exploiting (2), but the underlying input is DT signal  $\{u(kT_s)\}_{k=0}^{N-1}$  rather than CT signal  $\{u(t)\}_{t \leq NT_s}$ . Then the main problem can be addressed as follows:

- How to construct  $\{u(t)\}_{t \leq NT_s}$  from  $\{u(kT_s)\}_{k=0}^{N-1}$  to obtain the regularized estimator (3), and moreover, the closed form of  $\mathbf{\Sigma}_{gy_0}(\tau)$  and  $\mathbf{\Sigma}_{y_0}$ ?

The answer will be given in Section III.

## III. MAIN RESULT

In what follows, we first revisit how to construct  $\{u(t)\}_{t \leq NT_s}$  from  $\{u(kT_s)\}_{k=0}^{N-1}$  by using the input intersample and input past behaviors in Section III-A. Then, given such behaviors, we discuss the closed forms of  $\mathbf{\Sigma}_{gy_0}(\tau)$  and  $\mathbf{\Sigma}_{y_0}$  in Section III-B. For practical use, the results are extended to the unknown past behavior in Section III-C.

### A. From Sampled Input Signal to CT Input Signal

The construction of  $\{u(kT_s)\}_{k=0}^{N-1}$  is considered in two ways. On the one hand, the DT input signal needs to be converted into a CT input signal by using intersample behavior [15]. The typical intersample behaviors are

- zero-order hold (ZOH), i.e.,

$$\begin{aligned} u(t) &= \sum_{k=0}^{\infty} u(kT_s) \text{zoh}(t - kT_s) \text{ with} \\ \text{zoh}(t) &= 1_{(0, \infty)}(t) - 1_{(T_s, \infty)}(t), \end{aligned} \quad (5)$$

<sup>1</sup>Given a scalar function  $\xi(\cdot)$ , the vectorized scalar function  $\xi(\mathbf{t})$  outputs the vector  $[\xi(0), \dots, \xi((N-1)T_s)]^T$ . Similarly, this notation can be used for the scalar function with two vector inputs, e.g.,  $\xi(\mathbf{t}, \mathbf{t}^T)$ , which outputs a matrix.

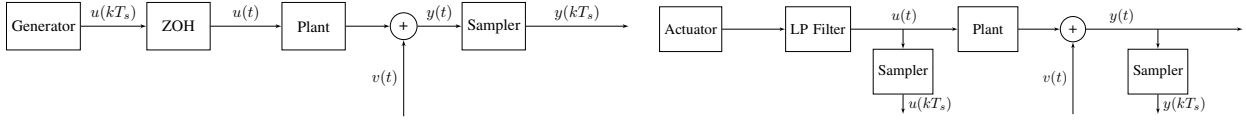


Fig. 1: Basic setup for ZOH (left) and BL (right) inputs in applications, where  $u(kT_s)$  and  $y(kT_s)$  are measured, and LP Filter denotes the low-pass filter for BL conditions. Refers the more general setup to [13, Chap. 13.2].

where  $1_*(t)$  is the indicator function, i.e., equal 1 when condition  $*$  is satisfied.

- band-limited (BL) under the Nyquist frequency, i.e., containing no frequencies on and above  $\pi/T_s$  rad/s. Further, if  $u(t)$  is periodic with period  $NT_s$  and BL under  $\pi/T_s$ , then it holds that

$$u(t) = \frac{1}{N} \sum_{|n| < \frac{N}{2}} \sum_{k=0}^{N-1} u(kT_s) e^{-j2\pi nk/N} e^{j2\pi nt/NT_s},$$

The intersample behavior is based on the measurement setup, see Fig.1, and thus it is assumed known in this paper.

On the other hand, the past input,  $u(t)$  with  $t < 0$ , needs to be specified in (4), and it can be inferred by assuming the past behavior [12, Sec. VIII]. The typical past behaviors are

- periodically appended (PA) with period  $NT_s$ , i.e.,

$$u(t - kNT_s) = u(t), \quad 0 \leq t < NT_s, k \in \mathbb{N}, \quad (6)$$

where PA in this paper shall always carry the information of periods  $NT_s$ ;

- zero appended (ZA), i.e.,

$$u(t) = 0, \quad \text{when } t < 0, \quad (7)$$

which is also known as the per-windowing approach [6, p.320].

The past behavior is often unknown, and the assumed PA and ZA behaviors are very likely to be inconsistent, leading to the estimation error. This error can be modeled in addition as the transient in Section III-C. For the moment, nonetheless, we assume the known intersample and past behaviors.

## B. Closed Forms for Known Intersample and Past Behaviors

Given the intersample and past behaviors,  $\{u(t)\}_{t \leq NT_s}$  can be constructed from  $\{u(kT_s)\}_{k=0}^{N-1}$ , and thus KRM can be applied. Then we consider the closed forms of  $\Sigma_{gy_0}(\tau)$  and  $\Sigma_{y_0}$  for different intersample and past behaviors. Since BL is contradictory to ZA, there are three different combinations to be considered: ZOH and PA, ZOH and ZA, BL and PA.

1) *ZOH and PA Input*: We first consider the ZOH input and PA input, respectively, and then their combination. On the one hand, if  $u(t)$  is ZOH, then the CT impulse response  $g(\tau)$  can be replaced by a DT model, see e.g. [15]. This leads to the following lemma.

**Lemma 2 (ZOH Input):** If  $u(t)$  is ZOH, then (4) can be rewritten as

$$\begin{cases} \Sigma_{y_0} = \sum_{s=1}^{\infty} \sum_{s'=1}^{\infty} u(\mathbf{t} - sT_s) u(\mathbf{t}^T - s'T_s) \kappa_{gd}(sT_s, s'T_s), \\ \Sigma_{gy_0}(\tau) = \sum_{s'=1}^{\infty} u(\mathbf{t}^T - s'T_s) \kappa_{gd}(\tau, s'T_s), \end{cases} \quad (8)$$

$$\begin{aligned} \kappa_{gd}(sT_s, s'T_s) &= \int_{(s-1)T_s}^{sT_s} \int_{(s'-1)T_s}^{s'T_s} \kappa_g(\tau, \tau') d\tau d\tau', \\ \kappa_{gd}(\tau, s'T_s) &= \int_{(s'-1)T_s}^{s'T_s} \kappa_g(\tau, \tau') d\tau', \quad s, s' \in \mathbb{N}_+. \end{aligned}$$

On the other hand, if  $u(t)$  is PA, then the CT impulse response  $g(\tau)$  can be replaced by a truncated CT model. This leads to the following lemma.

**Lemma 3 (PA Input):** If  $u(t)$  is PA with period  $NT_s$ , then (4) can be rewritten as

$$\begin{cases} \Sigma_{y_0} = \int_0^{NT_s} \int_0^{NT_s} u(\mathbf{t} - \tau) u(\mathbf{t}^T - \tau') \kappa_{gp}(\tau, \tau') d\tau d\tau', \\ \Sigma_{gy_0}(\tau) = \int_0^{NT_s} u(\mathbf{t}^T - \tau') \kappa_{gp}(\tau, \tau') d\tau', \end{cases} \quad (9)$$

$$\kappa_{gp}(\tau, \tau') = \sum_{n=0}^{\infty} \sum_{n'=0}^{\infty} \kappa_g(\tau + nNT_s, \tau' + n'NT_s),$$

$$\kappa_{gp}(\tau, \tau') = \sum_{n'=0}^{\infty} \kappa_g(\tau, \tau' + n'NT_s), \quad 0 \leq \tau, \tau' < NT_s.$$

However, from (8) and (9), relying alone on ZOH or PA does not suffice the closed forms of  $\Sigma_{gy_0}(\tau)$  and  $\Sigma_{y_0}$ . Then we consider the combination of them. If  $u(t)$  is PA and ZOH, then the CT impulse response  $g(\tau)$  can be replaced by a truncated DT model, leading to the following lemma.

**Lemma 4 (ZOH and PA Input):** If  $u(t)$  is ZOH and PA with period  $NT_s$ , then (4) can be rewritten as

$$\begin{cases} \Sigma_{y_0} = \sum_{s=1}^N \sum_{s'=1}^N u(\mathbf{t} - sT_s) u(\mathbf{t}^T - s'T_s) \kappa_{gdp}(sT_s, s'T_s), \\ \Sigma_{gy}(\tau) = \sum_{s'=1}^N u(\mathbf{t}^T - s'T_s) \kappa_{gdp}(\tau, s'T_s), \end{cases} \quad (10)$$

$$\kappa_{gdp}(s, s') = \sum_{n=0}^{\infty} \sum_{n'=0}^{\infty} \kappa_{gd}(sT_s + nNT_s, s'T_s + n'NT_s),$$

$$\kappa_{gdp}(\tau, s') = \sum_{n'=0}^{\infty} \kappa_{gd}(\tau, s'T_s + n'NT_s),$$

where  $\kappa_{gdp}$  and  $\kappa_{gdp}$  can also be induced from  $\kappa_{gp}$  and  $\kappa_{gp}$ . From Lemma 4, it is shown that the closed forms of  $\Sigma_{gy_0}(\tau)$  and  $\Sigma_{y_0}$  exist as long as the  $\kappa_{gdp}$  and  $\kappa_{gdp}$  have the closed forms. Nonetheless, their closed forms depend on the selection of the original kernel  $\kappa_g$ . Particularly, we consider a widely-used kernel for  $\kappa_g$  as an example.

**Example 1:** If  $\kappa_g(\tau, \tau')$  takes the form of the diagonal correlated (DC) kernel [16], described by

$$\kappa_g^{\text{DC}}(\tau, \tau') = \lambda e^{-\alpha(\tau+\tau')} e^{-\beta|\tau-\tau'|}, \quad (11)$$

where  $\alpha, \beta, \lambda$  are hyperparameters. Then we have

$$\begin{aligned}
\bullet \kappa_{gd}^{\text{DC}}(sT_s, s'T_s) &= \begin{cases} \lambda_1 \lambda e^{-\beta|s-s'|T_s - \alpha(s+s')T_s}, & \text{if } s \neq s' \\ \lambda_2 \lambda e^{-\alpha(s+s')T_s}, & \text{if } s = s' \end{cases}, \\
\lambda_1 &= \frac{(1 - e^{(\alpha-\beta)T_s})(1 - e^{(\alpha+\beta)T_s})}{\alpha^2 - \beta^2}, \\
\lambda_2 &= \frac{-2\alpha e^{(\alpha-\beta)T_s} - e^{2\alpha T_s}(\beta - \alpha) + \alpha + \beta}{\alpha^3 - \alpha\beta^2}, \\
\bullet \kappa_{gp}^{\text{DC}}(\tau, \tau') &= \lambda_3 \lambda e^{-\alpha(\tau+\tau') - \beta|\tau-\tau'|} + \lambda_3 \lambda_4 \lambda e^{-\alpha(\tau+\tau') + \beta(\tau-\tau')} \\
&\quad + \lambda_3 \lambda_4 \lambda e^{-\alpha(\tau+\tau') + \beta(\tau'-\tau)} \\
\lambda_3 &= \frac{1}{1 - e^{-2\alpha NT_s}}, \quad \lambda_4 = \frac{e^{-\beta NT_s - \alpha NT_s}}{1 - e^{-\alpha NT_s - \beta NT_s}}, \\
\bullet \kappa_{gdp}^{\text{DC}}(sT_s, s'T_s) &= \lambda_3 \kappa_{gd}^{\text{DC}}(sT_s, s'T_s) + \lambda_1 \lambda_3 \lambda_4 \lambda e^{-\alpha(s+s')T_s + \beta(s-s')T_s} \\
&\quad + \lambda_1 \lambda_3 \lambda_4 \lambda e^{-\alpha(s+s')T_s + \beta(s'-s)T_s},
\end{aligned}$$

where the closed forms of  $\kappa_{gd}$ ,  $\kappa_{gp}$ , and  $\kappa_{gdp}$  are left in Appendix A.1.

From Example 1, we have the following proposition.

**Proposition 1:** If the input signal is ZOH and PA, and if  $\kappa_g(\tau, \tau')$  is the DC kernel (11), then the closed forms of  $\Sigma_{gy_0}(\tau)$  and  $\Sigma_{y_0}$  exist as (10).

2) *ZOH and ZA Input:* If  $u(t)$  is ZA, then the CT impulse response  $g(\tau)$  can be truncated to  $NT_s$ , i.e.,

$$y_0(t) = \int_0^{NT_s} u(t-\tau)g(\tau) d\tau, \quad (12)$$

and moreover, If  $u(t)$  is ZOH and ZA, then the DT model can be truncated to  $N$ , leading to the following lemma.

**Lemma 5 (ZOH and ZA Input):** If  $u(t)$  is ZOH and ZA, then (4) can be rewritten as

$$\begin{cases} \Sigma_{y_0} = \sum_{s=1}^N \sum_{s'=1}^N u(\mathbf{t}-sT_s)u(\mathbf{t}^T-s'T_s)\kappa_{gd}(sT_s, s'T_s), \\ \Sigma_{gy_0}(\tau) = \sum_{s'=1}^N u(\mathbf{t}^T-s'T_s)\kappa_{gdp}(\tau, s'T_s), \end{cases} \quad (13)$$

where  $\kappa_{gd}$  and  $\kappa_{gdp}$  refer to (8).

**Proposition 2:** If the input signal is ZOH and ZA, and if  $\kappa_g(\tau, \tau')$  is the DC kernel (11), then the closed forms of  $\Sigma_{gy_0}(\tau)$  and  $\Sigma_{y_0}$  exist as (13).

3) *BL and PA Input:* If  $u(t)$  is BL and PA, then the corresponding result is complicated as summarized in the following lemma.

**Lemma 6 (PA Input and BL Input):** If  $u(t)$  is BL and PA, then (4) can be rewritten as

$$\begin{cases} \Sigma_{y_0} = \frac{1}{N^2} \sum_{|n| < \frac{N}{2}} \sum_{|n'| < \frac{N}{2}} e^{jn\omega_0 \mathbf{t}} e^{-jn'\omega_0 \mathbf{t}^T} U(n\omega_0) \overline{U}(n'\omega_0) \\ \quad \int_0^{NT_s} \int_0^{NT_s} \kappa_{gp}(\tau, \tau') e^{-jn\omega_0 \tau} e^{jn'\omega_0 \tau'} d\tau d\tau', \\ \Sigma_{gy}(\tau) = \frac{1}{N} \sum_{|n'| < \frac{N}{2}} e^{jn'\omega_0 \mathbf{t}^T} \overline{U}(n'\omega_0) \int_0^{NT_s} \kappa_{gdp}(\tau, \tau') e^{jn'\omega_0 \tau'} d\tau', \end{cases} \quad (14)$$

where  $\omega_0 = 2\pi/NT_s$ ,  $U(n\omega_0) = \sum_{k=0}^{N-1} u(kT_s)e^{-jn\omega_0 kT_s}$ , and  $\overline{U}(n\omega_0)$  is the complex conjugate of  $U(n\omega_0)$ .

Likewise to Example 1, if we choose the DC kernel (11), then  $\Sigma_{y_0}$  and  $\Sigma_{gy}(\tau)$  also have the closed form, but we skip it for limited space. Lastly, we have the following proposition.

**Proposition 3:** If the input signal is BL and PA, and if  $\kappa_g(\tau, \tau')$  is the DC kernel (11), then the closed forms of  $\Sigma_{gy_0}(\tau)$  and  $\Sigma_{y_0}$  exist as (14).

In summary, we have shown that all three different combinations of the intersample and past behaviors have the closed forms of  $\Sigma_{gy_0}(\tau)$  and  $\Sigma_{y_0}$ .

### C. Closed Forms for Unknown Past Behavior

In practice, the past behavior of the input signal is unknown, and then we need to make some assumptions on it and model the error in addition. As a result, a transient model is considered in parallel with the system model, see e.g. [12], [13], i.e.,

$$y(t) = y_p(t) + t_p(t) + v(t), \quad y_p(t) = \int_0^\infty u_p(t-\tau)g(\tau)d\tau, \quad (15)$$

$$t_p(t) = \int_0^\infty (u_p(t-\tau) - u(t-\tau))g(\tau)d\tau,$$

where  $u_p(t)$  is the input with assumed past behavior,  $u(t)$  is the actual input, and  $t_p(t)$  is the transient model.

Here we employ the Bayesian framework of KRM for better exposition, corresponding to Lemma 1. Let  $t_p(t)$  and  $g(\tau)$  are Gaussian processes and  $v(t)$  is the white Gaussian noise. This leads to a new MAP estimation as follows.

**Lemma 7:** Consider (15) with:

- 1)  $g(\tau)$  is a zero-mean GP with covariance function  $\kappa_g(\tau, \tau')$ ,
- 2)  $t_p(t)$  is a zero-mean GP with covariance function  $\kappa_t(t, t')$ , independent with  $g(\tau)$ ,
- 3)  $v(t)$  is a white Gaussian noise with variance  $\sigma^2$ , independent with  $g(\tau)$  and  $t_p(t)$ .

Given observation  $\mathbf{y} = [y(0), \dots, y((N-1)T_s)]^T$ , the MAP estimate of  $g(\tau)$  is

$$\begin{aligned} \hat{g}(\tau) &= \Sigma_{gy_p}(\tau)(\Sigma_{y_p} + \kappa_t(\mathbf{t}, \mathbf{t}^T) + \sigma^2 I_N)^{-1} \mathbf{y}, \\ \begin{cases} \Sigma_{y_p} = \int_0^\infty \int_0^\infty u_p(\mathbf{t}-\tau)u_p(\mathbf{t}^T-\tau')\kappa_g(\tau, \tau') d\tau d\tau', \\ \Sigma_{gy_p}(\tau) = \int_0^\infty u_p(\mathbf{t}^T-\tau')\kappa_g(\tau, \tau') d\tau'. \end{cases} \end{aligned} \quad (16)$$

It should be noted that  $\kappa_t$  is a kernel in analogy with  $\kappa_g$ . The design of  $\kappa_t$  can refer to [17, Sec. 5.3], but it does not affect the existence of the closed form of the estimator (16).

Then we are interested in the closed forms of the new estimator (16) (and also the new hyperparameter estimator), which depend on the closed form of  $\Sigma_{y_p}$  and  $\Sigma_{gy_p}(\tau)$ . It should be noted that  $\Sigma_{y_p}$  and  $\Sigma_{gy_p}(\tau)$  take the same forms as (4) with  $u_p(t)$  having the known intersample and past behaviors. Consequently, all results can be found as special cases in Section III-B.

## IV. SIMULATION

We run numerical simulations to compare KRM with SRIVC and ML/PEM. Due to the limited space, we only consider the typical case in practice [7]: the intersample behavior is ZOH and the past behavior is unknown.

### A. Data Generation

The following setup is the same as tutorial 1 in CONTSID 7.4 toolbox [18]. We consider the Rao–Garnier test system [14], whose transfer function is

$$G(s) = \frac{-6400s + 1600}{s^4 + 6s^3 + 408^2 + 416s + 1600}. \quad (17)$$

The input is a pseudo-random binary signal (PRBS) generated by CONTSID function `prbs(10, 7)` including 7167 samples in total, and the output is simulated by CONTSID

function `simc()`, where the sampling interval is  $T_s = 0.01$ , and the input is ZOH. Note that the past behavior is unknown. The additive noise is white Gaussian distributed with the signal-to-noise ratio (SNR) being 10 dB. Lastly, the 3001st to 4000th input and output are saved in one trail with  $N = 1000$ , and 200 Monte Carlo (MC) trails are run with different inputs and noise realizations for one data bank.

To enrich the benchmark, we also choose other values of  $T_s$  and  $N$ . Specifically, we generate four data banks D1-D4:

D1:  $T_s = 0.01$  and  $N=1000$ , such that  $N \cdot T_s = 10$ .

D2:  $T_s = 0.05$  and  $N=200$ , such that  $N \cdot T_s = 10$ .

D3:  $T_s = 0.1$  and  $N=100$ , such that  $N \cdot T_s = 10$ .

D4:  $T_s = 0.1$  and  $N=1000$ , such that  $N \cdot T_s = 100$ .

It is shown in [19] that the normal sampling interval for system (17) is  $T_s = 0.05$ , implying that  $T_s = 0.01$  in D1 is over-sampled, and  $T_s = 0.1$  in D3/D4 is under-sampled.

### B. Estimator Setup

The tested estimators include

- SRIVC, implemented by `srivc()` in CONTSID Toolbox [18];
- PEM, implemented by `tfest()` in MATLAB System Identification Toolbox [7];
- KRM, implemented by (16) with  $\Sigma_{y_p}$  and  $\Sigma_{a_{gy_p}}$  being (13) and kernel being the DC kernel (11).

Specifically, SRIVC and ML/PEM need to select the orders of the numerator and denominator from [1, 9] and [2, 10], respectively, with a constraint of the positive relative degree. For both SRIVC and ML/PEM, the model order selection is based on the Young information criterion (YIC) or Akaike information criterion (AIC), implemented by `selcstruc()` in CONTSID Toolbox with 'Algo' being 'srivc'. Besides, the true model orders are also used as the oracle (OR). As for KRM,  $\kappa_t$  is chosen to be  $\alpha_t \kappa_g$  with  $\alpha_t > 0$  being an extra hyperparameter. The hyperparameter estimation is implemented by the Empirical Bayes method with MATLAB function `MultiStart()` with `fmincon()`, and the number of runs is 5 times the number of the hyperparameters.

### C. Evaluation Criteria

The evaluation criteria depend on the goal of the model, e.g. prediction and control design. For the goal of prediction, the model is assessed by comparing the predicted output and the true noiseless output in the validation data:

$$\text{FIT}_y = 100 \left( 1 - \left[ \frac{\sum_{k=1}^{1000} |y_0(kT_s) - \hat{y}(kT_s)|^2}{\sum_{k=1}^{1000} |y_0(kT_s) - \bar{y}_0|^2} \right]^{\frac{1}{2}} \right),$$

where  $\bar{y}_0 = \sum_{k=1}^{1000} y_0(kT_s)$ , and the true past input are provided for  $\hat{y}$ . For the goal of control design, the model is assessed by comparing the estimated and true impulse response over-sampled at  $\mathcal{X}_e = \{0.01/50 : 0.01/50 : 10\}$ :

$$\text{FIT}_g = 100 \left( 1 - \left[ \frac{\sum_{\tau \in \mathcal{X}_e} |g_0(\tau) - \hat{g}(\tau)|^2}{\sum_{\tau \in \mathcal{X}_e} |g_0(\tau) - \bar{g}_0|^2} \right]^{\frac{1}{2}} \right),$$

where  $\bar{g}_0 = \sum_{\tau \in \mathcal{X}_e} g_0(\tau)$ . The evaluation criteria are independent of the choices of  $T_s$  and  $N$ .

TABLE I: Mean and standard deviation (std) of FIT.

Estimate	Mean <sub>std</sub> of FIT <sub>g</sub>			
	D1	D2	D3	D4
KRIVC(YIC)	66.45 <sub>54.97</sub>	30.10 <sub>57.27</sub>	-59.40 <sub>82.11</sub>	32.43 <sub>49.77</sub>
KRIVC(AIC)	66.88 <sub>42.04</sub>	22.03 <sub>67.27</sub>	-47.05 <sub>107.71</sub>	69.19 <sub>33.24</sub>
KRIVC(OR)	<b>97.15</b> <sub>0.88</sub>	53.68 <sub>48.56</sub>	-18.62 <sub>60.76</sub>	<b>84.07</b> <sub>17.21</sub>
PEM(YIC)	69.29 <sub>53.32</sub>	34.07 <sub>73.43</sub>	-14.07 <sub>68.51</sub>	43.63 <sub>56.03</sub>
PEM(AIC)	58.40 <sub>67.07</sub>	31.54 <sub>64.83</sub>	5.88 <sub>58.08</sub>	61.06 <sub>37.33</sub>
PEM(OR)	96.65 <sub>1.01</sub>	59.72 <sub>31.21</sub>	25.07 <sub>54.58</sub>	71.10 <sub>17.14</sub>
KRM	88.73 <sub>1.16</sub>	<b>63.06</b> <sub>4.62</sub>	<b>45.34</b> <sub>14.75</sub>	74.06 <sub>4.85</sub>
Estimate	Mean <sub>std</sub> of FIT <sub>y</sub>			
	D1	D2	D3	D4
SRIVC(YIC)	69.47 <sub>67.20</sub>	76.15 <sub>38.45</sub>	38.33 <sub>52.04</sub>	49.05 <sub>51.34</sub>
SRIVC(AIC)	93.67 <sub>14.13</sub>	85.30 <sub>21.73</sub>	62.21 <sub>38.52</sub>	90.00 <sub>27.69</sub>
SRIVC(OR)	<b>97.51</b> <sub>0.79</sub>	<b>92.04</b> <sub>7.05</sub>	52.00 <sub>61.79</sub>	<b>96.57</b> <sub>4.05</sub>
PEM(YIC)	70.17 <sub>64.20</sub>	49.00 <sub>87.53</sub>	-122.25 <sub>374.22</sub>	61.89 <sub>57.06</sub>
PEM(AIC)	56.49 <sub>71.71</sub>	40.33 <sub>103.14</sub>	-12.58 <sub>208.55</sub>	81.82 <sub>37.85</sub>
PEM(OR)	97.11 <sub>0.87</sub>	90.43 <sub>7.10</sub>	56.37 <sub>53.98</sub>	94.93 <sub>2.20</sub>
KRM	90.37 <sub>1.04</sub>	86.03 <sub>1.96</sub>	<b>72.74</b> <sub>6.06</sub>	94.10 <sub>0.69</sub>

### D. Results and Findings

The boxplots of FIT<sub>g</sub> and FIT<sub>y</sub> are shown in Fig. 2, and the mean and standard deviation (std) of FIT<sub>g</sub> and FIT<sub>y</sub> are tabulated in Table I. The following tendency is consistent with our expectations:

- The larger  $N$  improves both FIT<sub>g</sub> and FIT<sub>y</sub> in terms of the mean and std.
- The larger  $T_s$  deteriorates FIT<sub>g</sub> in terms of the mean and std, while its influence on FIT<sub>y</sub> is relatively weak.

Moreover, we have the following observations on estimates:

- for the estimator's robustness in terms of the std, KRM is more robust than SRIVC and ML/PEM, and they are equally robust in D1 (larger sample size  $N$ ) with the true model order provided.
- for the estimator's accuracy in terms of the mean, KRM is more accurate than SRIVC and ML/PEM in D3 (smaller sample size  $N$ ), and, if the true model order is unknown, then KRM is almost no worse than SRIVC and ML/PEM.

### E. Conclusion

This work proposes the kernel-based regularization method for continuous-time system identification from the sampled data. The closed forms of the estimators are demonstrated when the input has certain combinations of the inter-sample and past behaviors. For practical use, the result can be extended to when the input has unknown past behavior. According to the numerical simulations, the proposed method has demonstrated better robustness compared to the state-of-the-art methods, SRIVC and ML/PEM, and the proposed method also has better accuracy for the small sample size.

### REFERENCES

- [1] P. Young. Parameter estimation for continuous-time models - a survey. *Automatica*, 17(1):23–39, 1981.
- [2] H. Unbehauen and G.P. Rao. Continuous-time approaches to system identification—a survey. *Automatica*, 26(1):23–35, 1990.
- [3] H. Garnier. Direct continuous-time approaches to system identification. overview and benefits for practical applications. *European Journal of control*, 24:50–62, 2015.
- [4] P. Young and A. Jakeman. Refined instrumental variable methods of recursive time-series analysis part iii. extensions. *International Journal of Control*, 31(4):741–764, 1980.

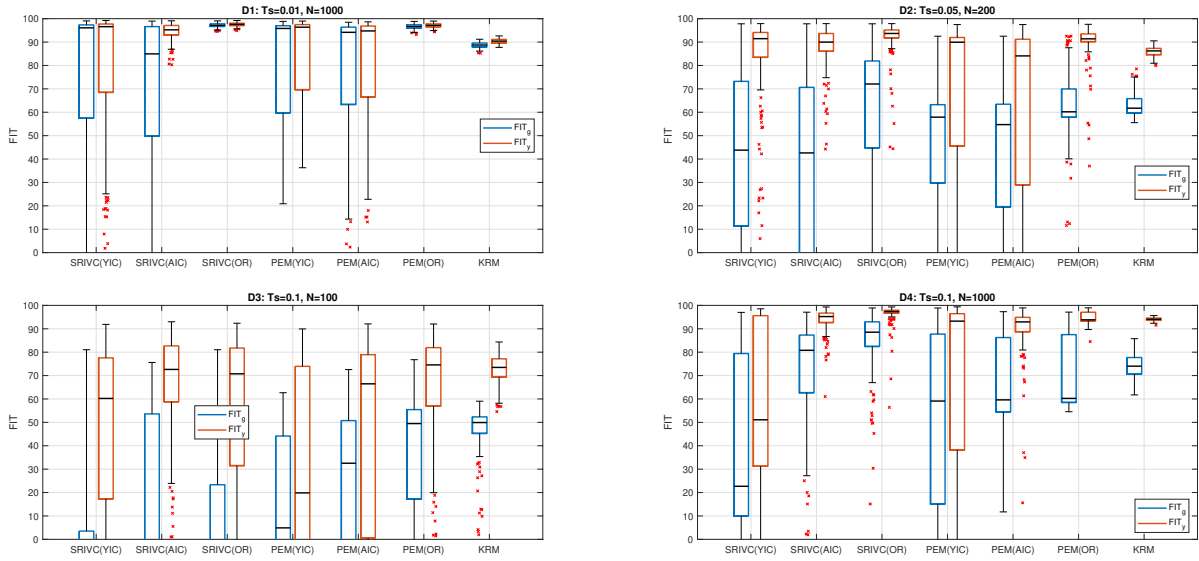


Fig. 2: The boxplots of  $FIT_g$  (blue) and  $FIT_y$  (red) for 200 MC trials. The mean and standard deviation refer to Table I.

- [5] H. Garnier, L. Wang, and P.C. Young. Direct identification of continuous-time models from sampled data: Issues, basic solutions and relevance. In *Identification of continuous-time models from sampled data*, pages 1–29. Springer, 2008.
- [6] L. Ljung. *System Identification - Theory for the User*. Prentice-Hall, Upper Saddle River, N.J., 2nd edition, 1999.
- [7] L. Ljung. Experiments with identification of continuous time models. *IFAC Proceedings Volumes*, 42(10):1175–1180, 2009.
- [8] L. Ljung, T. Chen, and B. Mu. A shift in paradigm for system identification. *International Journal of Control*, 93(2):173–180, 2020.
- [9] G. Pillonetto, F. Dinuzzo, T. Chen, G. De Nicolao, and L. Ljung. Kernel methods in system identification, machine learning and function estimation: A survey. *Automatica*, 50(3):657–682, 2014.
- [10] M. Scandella, M. Mazzoleni, S. Formentin, and F. Previdi. Kernel-based identification of asymptotically stable continuous-time linear dynamical systems. *International Journal of Control*, 95(6):1668–1681, 2022.
- [11] G. Pillonetto and G. De Nicolao. A new kernel-based approach for linear system identification. *Automatica*, 46(1):81–93, 2010.
- [12] L. Ljung. State of the art in linear system identification: Time and frequency domain methods. In *Proceedings of the 2004 American Control Conference*, volume 1, pages 650–660. IEEE, 2004.
- [13] R. Pintelon and J. Schoukens. *System identification: a frequency domain approach*. John Wiley & Sons, 2012.
- [14] H. Garnier and P.C. Young. The advantages of directly identifying continuous-time transfer function models in practical applications. *International Journal of Control*, 87(7):1319–1338, 2014.
- [15] J. Schoukens, R. Pintelon, and H. Van Hamme. Identification of linear dynamic systems using piecewise constant excitations: Use, misuse and alternatives. *Automatica*, 30(7):1153–1169, 1994.
- [16] T. Chen, H. Ohlsson, and L. Ljung. On the estimation of transfer functions, regularizations and gaussian processes—revisited. *Automatica*, 48(8):1525–1535, 2012.
- [17] J. Lathar and T. Chen. Transfer function and transient estimation by Gaussian process regression in frequency domain. *Automatica*, 52:217–229, 2016.
- [18] H. Garnier, M. Gilson, H. Muller, and F. Chen. A new graphical user interface for the conssid toolbox for matlab. *IFAC-PapersOnLine*, 54(7):397–402, 2021.
- [19] H. Garnier, M. Mensler, and A. Richard. Continuous-time model identification from sampled data: implementation issues and performance evaluation. *International Journal of Control*, 76(13):1337–1357, 2003.

## APPENDIX

### A.1. Complementary Materials for Example 1

$$\bullet \kappa_{ggd}^{DC}(\tau, s'; \eta) = \begin{cases} \text{EXP1,} & \text{if } s' - 1 < \tau/T_s \leq s' \\ \text{EXP2,} & \text{if } \tau/T_s > s', \\ \text{EXP3,} & \text{if } \tau/T_s \leq s' - 1, \end{cases},$$

$$\bullet \kappa_{gdp}^{DC}(\tau, \tau'; \eta) = \frac{1}{1 - e^{-(\alpha+\beta)NT_s}} M_1 - \frac{1 - e^{-(\alpha+\beta)NT_s C_1}}{1 - e^{-(\alpha+\beta)NT_s}} M_1 + \frac{1 - e^{-(\alpha-\beta)NT_s C_1}}{1 - e^{-(\alpha-\beta)NT_s}} M_2$$

$$M_1 = \lambda e^{-\alpha(\tau+\tau')-\beta(\tau'-\tau)}, \quad M_2 = \lambda e^{-\alpha(\tau+\tau')-\beta(\tau-\tau')},$$

$$\bullet \kappa_{gdp}^{DC}(\tau, s'; \eta) = \begin{cases} \text{EXP4,} & \text{if } s' - 1 < \text{mod}(\frac{\tau}{T_s}, N) \leq s' \\ \text{EXP5,} & \text{otherwise,} \end{cases},$$

$$\text{EXP1} = \frac{\lambda}{\alpha^2 - \beta^2} \left( (\beta - \alpha) e^{-\alpha(\tau+s'T_s)-\beta(s'T_s-\tau)} - 2\beta e^{-2\alpha\tau} + (\alpha + \beta) e^{-\alpha(\tau+(s'-1)T_s)-\beta(\tau-(s'-1)T_s)} \right),$$

$$\text{EXP2} = \frac{\lambda}{\alpha - \beta} \left( e^{-\alpha(\tau+(s'-1)T_s)} e^{-\beta|\tau-(s'-1)T_s|} - e^{-\alpha(\tau+s'T_s)} e^{-\beta|\tau-s'T_s|} \right),$$

$$\text{EXP3} = \frac{\lambda}{\alpha + \beta} \left( e^{-\alpha(\tau+(s'-1)T_s)} e^{-\beta|\tau-(s'-1)T_s|} - e^{-\alpha(\tau+s'T_s)} e^{-\beta|\tau-s'T_s|} \right),$$

$$\text{EXP4} = \lambda e^{-\alpha(\tau+s'T_s)} \left( \frac{1}{1 - e^{-(\alpha+\beta)NT_s}} S_5 - \frac{1 - e^{-(\alpha+\beta)NT_s C_2}}{1 - e^{-(\alpha+\beta)NT_s}} S_1 + \frac{1 - e^{-(\alpha-\beta)NT_s C_2}}{1 - e^{-(\alpha-\beta)NT_s}} S_2 - \frac{1 - e^{-(\alpha+\beta)NT_s C_3}}{1 - e^{-(\alpha+\beta)NT_s}} S_3 + \frac{1 - e^{-(\alpha-\beta)NT_s C_3}}{1 - e^{-(\alpha-\beta)NT_s}} S_4 \right)$$

$$\text{EXP5} = \lambda e^{-\alpha(\tau+s'T_s)} \left( \frac{1}{1 - e^{-(\alpha+\beta)NT_s}} S_5 - \frac{1 - e^{-(\alpha+\beta)NT_s C_2}}{1 - e^{-(\alpha+\beta)NT_s}} S_5 + \frac{1 - e^{-(\alpha-\beta)NT_s C_3}}{1 - e^{-(\alpha-\beta)NT_s}} S_6 \right),$$

$$\begin{aligned}
C_1 &= \text{ceil}[(\tau - \tau')/(NT_s)], C_2 = \text{ceil}[(\tau/T_s - s')/N], \\
C_3 &= \text{ceil}[(\tau/T_s - s' + 1)/N], \\
S_1 &= \frac{e^{(\alpha+\beta)T_s} - e^{-(\alpha+\beta)(\text{mod}(\tau, NT_s) - s'T_s)}}{\alpha + \beta} e^{-\beta(s'T_s - \tau)}, \\
S_2 &= \frac{e^{(\alpha-\beta)T_s} - e^{-(\alpha-\beta)(\text{mod}(\tau, NT_s) - s'T_s)}}{\alpha - \beta} e^{-\beta(\tau - s'T_s)}, \\
S_3 &= \frac{-1 + e^{-(\alpha+\beta)(\text{mod}(\tau, NT_s) - s'T_s)}}{\alpha + \beta} e^{-\beta(s'T_s - \tau)}, \\
S_4 &= \frac{-1 + e^{-(\alpha-\beta)(\text{mod}(\tau, NT_s) - s'T_s)}}{\alpha - \beta} e^{-\beta(\tau - s'T_s)}, \\
S_5 &= \frac{e^{(\alpha+\beta)T_s} - 1}{\alpha + \beta} e^{-\beta(s'T_s - \tau)}, S_6 = \frac{e^{(\alpha-\beta)T_s} - 1}{\alpha - \beta} e^{-\beta(\tau - s'T_s)}.
\end{aligned}$$